Environmental Advances 7 (2022) 100171

Contents lists available at ScienceDirect

Environmental Advances

journal homepage: www.sciencedirect.com/journal/environmental-advances

Effects of the COVID-19 shutdown on spatial and temporal patterns of air pollution in New York City

Masha Pitiranggon [a,*], Sarah Johnson [a], Christopher Huskey [a], Holger Eisl [b], Kazuhiko Ito [a]

[a] New York City Department of Health and Mental Hygiene, Bureau of Environmental Surveillance and Policy, 125 Worth Street, Third Fl. CN-34E, New York, New York 10013, United States

[b] Barry Commoner Center for Health and the Environment, Queens College, City University of New York, Flushing, New York 11367, United States

ARTICLE INFO

Keywords:
Particulate matter
Nitrogen dioxide
Policy
Difference-in-difference estimation
Land use regression

ABSTRACT

Using spatially- and temporally-resolved data from the New York City Community Air Survey (NYCCAS) and the New York State (NYS) Department of Environmental Conservation (DEC) network, we characterized changes in fine particulate matter ($PM_{2.5}$) and nitrogen dioxide (NO_2) following the COVID-19 shutdown in NYC (3/20/20 – 6/7/20). Difference-in-difference analysis of $PM_{2.5}$ and NO_2 measured at 93 sites were used to estimate the change in citywide pollution attributable to the shutdown. We also quantified how these pollutant changes varied among different demographic groups using difference-in-difference analyses stratified by neighborhood poverty levels and rates of $PM_{2.5}$-attributable health outcomes. Spatial patterns of $PM_{2.5}$ and NO_2 were interpolated across NYC by fitting land-use regression models to measurements at the 93 sites. Weather conditions and emission source trends were analyzed to determine the potential effects of meteorology and specific emission sources on the observed pollution changes. We estimate that citywide average $PM_{2.5}$ and NO_2 decreased by approximately 25% and 29%, respectively, due to the shutdown. Weather readings show little evidence that meteorology biased our results in the direction of our findings. Data on major sources of $PM_{2.5}$ and NO_2 pollution suggests that decreased vehicle traffic and commercial cooking contributed to declines in air pollution during this period. Pollution reductions occurred disproportionately in the city's central business district (CBD), with smaller changes in other areas of the city, such as those with the highest burden of air pollution-related health impacts. These findings emphasize the need to target pollution sources in communities that suffer the greatest from pollution exposure in the design of equitable environmental health policy.

1. Introduction

To mitigate the COVID-19 pandemic, many governments across the world implemented "lockdown" measures to reduce the spread of the disease. On March 20, 2020, the governor of New York issued the "New York State on Pause" (NY Pause) executive order, which closed all non-essential businesses in the state by March 22, 2020. NY Pause also included a stay-at-home order, directing individuals to limit outdoor recreational activities and use of public transportation (NYS Department of Health, 2020). Though indoor dining was banned during the shutdown, restaurants and bars were allowed to continue offering takeout and delivery (Gold and Stevens 2020). On June 8, 2020, NYC became the last region in the state to meet the requirements to start the first phase of reopening, which allowed nonessential business to resume in the following industries: construction, retail (limited to delivery, curbside, and in-store pickup), manufacturing, wholesale trade, and agriculture, forestry, fishing and hunting (Gold and Stevens, 2020, New York State, 2021).

The changes in economic activity resulting from NY Pause had effects that cascaded across numerous aspects of everyday life, including air pollution emissions.

Other studies have reported decreased air pollution in NYC and elsewhere following lockdown measures. Perrera et al. (2021) estimated a 23% decline in $PM_{2.5}$ and a 34% decline in NO_2 pollution during the shutdown in NYC compared to the average concentration for the same months in 2015-2018. Fu et al. (2020) estimate ~28% decrease in NO_2 and $PM_{2.5}$ AQIs in NYC during the lockdown period compared to the same period in 2019. A study of changes in $PM_{2.5}$, PM_{10}, NO_2, and CO pollution in India reported reductions of up to 68% (Ahmedabad), 71% (Delhi), 87% (Bangalore), and 63% (Nagpur) for $PM_{2.5}$, PM_{10}, NO_2, and

* Corresponding author.
E-mail address: mpitiranggon@health.nyc.gov (M. Pitiranggon).

https://doi.org/10.1016/j.envadv.2022.100171
Received 28 September 2021; Received in revised form 15 December 2021; Accepted 11 January 2022
Available online 13 January 2022

CO, respectively, during the lockdown period compared to the pre-lockdown period (Navinya et al. 2020). In a study of pollution in Wuhan, China, Chen et al. (2020) attribute a 22.8 μg/m^3 decline in NO_2 and a 1.4 μg/m^3 decline in $PM_{2.5}$ to the large-scale quarantines implemented in response to the COVID-19 pandemic. Venter et al. (2020) estimate 31% and 60% reductions in population-weighted particulate matter and NO_2 in 34 countries, attributing most of the changes in NO_2 to declines in transportation sector emissions.

Though any public health benefits associated with air pollution reductions during the COVID-19 shutdown are eclipsed by the enormous human cost of the pandemic, the abrupt changes in activity have allowed us to evaluate the potential effect of future pollution regulations. Exposure to $PM_{2.5}$ has long been linked to adverse respiratory and cardiovascular health outcomes and excess premature deaths (Alexeeff et al. 2021, Orellano et al. 2020, US Environmental Protection Agency (USEPA) 2019). NO_2, as well, has been implicated as a contributor to mortality, hospital admissions, and respiratory diseases (Atkinson et al. 2018, Costa et al. 2014, US Environmental Protection Agency, 2016). Some of the diseases associated with long-term $PM_{2.5}$ and NO_2 exposure, such as chronic obstructive pulmonary disease (COPD), heart failure, hypertension, and diabetes (US Environmental Protection Agency, 2016, US Environmental Protection Agency (USEPA) 2019), have also been associated with higher risk of mortality and severe illness among COVID-19 patients (Cho et al. 2021, Song et al., 2021). Additionally, recent studies have observed a correlation between long-term exposures to $PM_{2.5}$ and NO_2 and COVID-19 mortality and severity (Bozack et al. 2021, Liang et al. 2020, Wu et al 2020).

While other studies have reported decreased air pollution in NYC and elsewhere following lockdown measures (Adams 2020, Berman and Ebisu 2020, Briz-Redon et al. 2021, Chen et al. 2020, Fu et al. 2020, He et al. 2020, Ju et al. 2021, Kerr et al. 2021, Le et al. 2020, Navinya et al. 2020, Perera et al. 2021, Venter et al. 2020), none that we know of have examined lockdown-related changes in ground-level air pollution with the spatial resolution afforded by the dense network of NYCCAS air monitors. We interpolate spatial patterns of $PM_{2.5}$ and NO_2 in the winter, spring, summer, and fall seasons of 2019 and 2020 across NYC by fitting land-use regression models to measurements at 93 NYCCAS sites. Unlike other studies that have used air pollution data from federal regulatory monitors to evaluate the effects of NY Pause on air pollution in NYC (Perera et al. 2021, Shehzad et al. 2021, Zangari et al. 2020), this study implements difference-in-difference estimation and analysis of local meteorology to infer the extent to which the COVID-19 shutdown caused the observed changes in air pollution, apart from external factors, such as seasonality and long-term trends. Furthermore, use of the high density NYCCAS data produces an estimate of changes caused by the shutdown that is more representative of changes across the entire city than analyses using the sparser regulatory network. The NYCCAS dataset also enabled us to quantify how changes in air quality during the shutdown varied among neighborhoods with different rates of poverty and air pollution-attributable health outcomes. At the time of writing, ours is the only study that examines these changes during the entire NY Pause period (March 20th – June 7th, 2020), as well as the period after reopening, including fall 2020 when COVID-19 cases resurged in NYC. Together with historic and real-time or near real-time data on major local pollution sources, this information has allowed us to parse out the potential effects of individual sources on observed changes in air pollution.

2. Materials and methods

2.1. Hourly air pollution data

NYCCAS hourly $PM_{2.5}$ measurements were collected by pDR-1500 $PM_{2.5}$ aerosol monitors (Thermo Fisher Scientific, Waltham, MA) in a temperature-controlled cell. These monitors are predominately placed at high-traffic locations, such as bridge and tunnel entrances in the CBD. $PM_{2.5}$ data collected from these sensors were aggregated hourly and adjusted based on the 24-hour air temperature measurements at LaGuardia Airport to better align readings to the $PM_{2.5}$ Federal Reference Method (FRM) monitors located on the Queens College campus in Queens, NY. In addition to hourly $PM_{2.5}$ data collected by NYCCAS, we obtained hourly $PM_{2.5}$ and NO_2 measurements from the NYS DEC (NYS Department of, 2021). Details of the NYS DEC monitoring network and sampling methods are described elsewhere (Civerolo et al. 2017, Schwab et al. 2006). The locations of all hourly monitoring sites used in this study are shown in Fig. S1a. Additionally, Fig. 1 displays the study area with select points of interest.

2.2. Spatially-resolved integrated air pollution data

The study design and analytical protocols for the NYCCAS integrated monitoring network are described in detail elsewhere (Matte et al. 2013, NYC Department of Health and Mental Hygiene (NYC DOHMH) 2021a). Briefly, NYCCAS started in December 2008 and runs on annual winter to fall cycles (i.e., NYCCAS Year 1 spanned December 16, 2008 to December 1, 2009). Monitoring sites were chosen to cover a wide range of land-use characteristics, including traffic and density of built space, with good geographic distribution across the city. Integrated two-week $PM_{2.5}$ samples were collected on Teflon filters and gravimetrically analyzed for $PM_{2.5}$ mass. Integrated two-week NO_2 samples were collected on passive samplers (Ogawa & Co. USA, Pompano Beach, FL, USA) before water-based extraction and colorimetric analysis. Since most sites are sampled for only one two-week session per season, with the exception of the three continuously monitored reference sites, we performed temporal adjustment according to the method described in a prior study (Ito et al. 2016). Briefly, generalized additive models (GAM) were fit to predict season-specific concentrations for each pollutant in each year by site ID and a smooth function of the unique session ID assigned to each two-week session using penalized splines with up to six degrees of freedom, which accounts for the six two-week sampling sessions in a NYCCAS season. Because the reference sites make up the majority of the observations, their inclusion in the model underscores the temporal patterns of air pollution throughout the season. Locations of the integrated sampling sites included in this study are shown in Figure S1b, and Table S1 shows the exact dates of NYCCAS sampling seasons in 2016 - 2020. GAM was performed using the mgcv package in R version 3.5.2 (R Foundation for Statistical Computing, Vienna, Austria).

2.3. Emissions indicators and weather data

To determine the potential causes of observed changes in pollution, we analyzed local emission sources and meteorology. Weather measurements from LaGuardia Airport (LGA) were obtained from the National Weather Service and the National Oceanic and Atmospheric Administration. Daily average temperature, relative humidity, precipitation, and wind speeds in NYC were analyzed to determine if meteorology had a significant effect on the observed pollution changes. The pollution sources we examined were chosen based on emissions indicators that were found to be important in land-use regression (LUR) modeling of the NYCCAS integrated $PM_{2.5}$ and NO_2 data (NYC Department of Health and Mental Hygiene (NYC DOHMH) 2021c). These emissions indicators were developed and described elsewhere (Clougherty et al. 2013, NYC Department of Health and Mental Hygiene (NYC DOHMH) 2021a). The data sources for these emissions indicators include: New York Metropolitan Transportation Council (NYMTC) traffic data, the U.S. Environmental Protection Agency's (USEPA) National Emissions Inventory, NYC Department of City Planning Primary Land Use Tax Lot Output (PLUTO) buildings data, and the NYC Fire Department. Table 1 summarizes the data sources for the emissions indicators used in our LUR models.

In recent years, the following emissions indicators were found to be

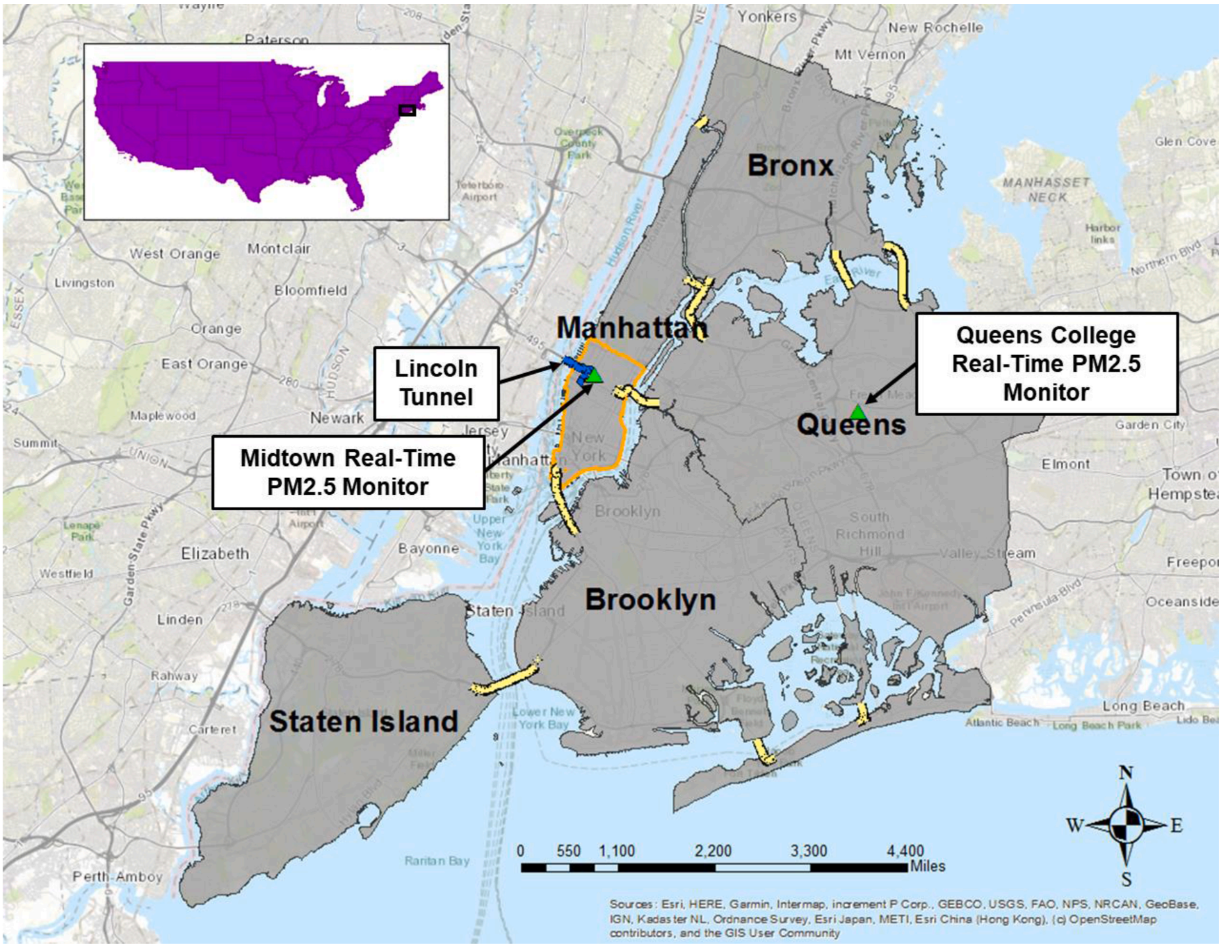

Fig. 1. Map of the study area along with select real-time PM2.5 and traffic speed/volume monitoring sites. The central business district (CBD) is outlined in orange and MTA Bridges and Tunnels are indicated by yellow segments outlined in black. The real-time PM2.5 monitors are displayed as green triangles and the Lincoln Tunnel is lined in blue.

significant predictors of $PM_{2.5}$: (1) number of permitted commercial char broilers less the number of precipitators within 1000m, (2) $PM_{2.5}$ emissions from heat and hot water boilers in buildings within 1000m, (3) area of industrial land use within 1000m, and (4) traffic density weighted by relative $PM_{2.5}$ emissions rates by vehicle type within 250m. The following emissions indicators are important predictors of NO_2: (1) area of industrial land use within 1000m, (2) traffic density weighted by relative NO_x emissions by vehicle type within 100m, (3) whether a site is located within 100 feet of a bus route, (4) area of interior building space within 1000m, and (5) percent impervious surface within 100m. These sources were quantified at 100m x 100m grid cells across NYC, and smoothed surfaces of calculated source densities were produced using inverse distance weighting (IDW) (Fig. S2). These emissions indicators are broadly related to three pollution sources: fuel burning for building heat and hot water, commercial cooking, and traffic. We examined real-time and near-real-time data on emission source activity to understand how these emissions changed across NYC during the shutdown. To elucidate changes in traffic, we analyzed traffic speed measurements obtained from the NYC Department of Transportation (DOT) (NYC Department of Transportation (NYC DOT) 2021), as well as traffic volume data reported by the Metropolitan Transportation Authority (MTA) Bridges and Tunnels (Metropolitan Transportation Authority 2021). Additionally, we examined heating fuel consumption (US Energy Information Administration 2020) and small business activity (Opportunity Insights 2021) before, during, and after the shutdown.

2.4. Difference-in-difference estimation

Difference-in-difference (DiD) estimation was used to calculate the change in citywide average pollutant concentrations that could be attributed to the COVID-19 shutdown. The DiD method is described in detail elsewhere (Dimick and Ryan 2014, Lechner 2010). Briefly, DiD is a causal inference method that is used to evaluate the effect of an intervention by comparing changes in an outcome over time between a group that was exposed to the intervention (intervention group) and one that was not (control group). A key component of the DiD study design is that the control group experiences the same non-intervention-related trends as the intervention group, thereby making it possible to isolate the effect of the intervention. We implemented the DiD approach in regression modeling, where the effect of intervention is estimated by the interaction between the time variable (pre- or post-intervention) and treatment group indicator (intervention or control).

In this study, the DiD method was employed to separate seasonal and long-term trends in $PM_{2.5}$ and NO_2 concentrations from the effect of the COVID-19 shutdown in NYC. Since the shutdown occurred at approximately the transition from winter to spring, we assigned the NYCCAS winter (12/4/2018 – 3/12/19) and spring (3/12/2019 – 6/4/2019) sessions of 2019 as the control group with the winter (12/3/2019 – 3/10/2020) and spring (3/10/2020 – 6/2/2020) sessions of 2020 as the intervention group. The basis of this approach being that the changes in pollutant concentrations from winter to spring observed in 2019 capture the same effects of seasonality and long-terms trends (i.e., due to the effect of prior pollution regulation) on pollutant changes in 2020. Four

Table 1
Data sources and interpretation of emissions indicators used in $PM_{2.5}$ and NO_2 land-use regression models.

Emissions indicator	Data source	Associated sources and interpretation
Number of permitted commercial char broilers less the number of precipitators within 1000m	NYC Fire Department	Emissions from commercial cooking
Area of industrial land use within 1000m	NYC Department of City Planning Primary Land Use Tax Lot Output (PLUTO™) data, 2016	Emissions from trucks idling and traveling through industrial areas and industrial combustion equipment
Traffic density weighted by relative PM2.5 emissions rates by vehicle type within 250m	NYMTC traffic data 2010; county level on road mobile emissions by vehicle class from National Emissions Inventory, 2017	PM2.5 from different classes of on-road motor vehicles allocated using vehicle miles traveled by vehicle class.
Traffic density weighted by relative NOx emissions rates by vehicle type within 100m	NYMTC traffic data 2010; county level on road mobile emissions by vehicle class from National Emissions Inventory, 2017	Total NOx emissions from different classes of on-road motor vehicles allocated using vehicle miles traveled by vehicle class.
Location on a bus route (whether or not site is within 100 ft of a bus route)	NYC Department of Transportation (DOT), 2020	Emissions from buses and other vehicles on busy roadways - indicator of traffic congestion
Area of interior building space within 1000m	NYC Department of City Planning Primary Land Use Tax Lot Output (PLUTO™) data, 2016	Combustion of heating oil and natural gas
Percent impervious surface within 100m	United States Geological Survey, 2016	Emissions of motor vehicles on paved roadways

periods of study (Winter 2018 - 2019, Spring 2019, Winter 2019 - 2020, Spring 2020) were included in the DiD models, comprising the respective seasonal averages of $PM_{2.5}$ and NO_2 measurements from the NYCCAS integrated monitors; this dataset is described in section 2.2. The seasonal average $PM_{2.5}$ and NO_2 values were log-transformed before performing DiD regression to correct for their right-skewed distributions and to coerce model residuals into an approximately normal distribution. Thus, the model produces the percent change in geometric means of each pollutant, given by the exponential of β_3 in the following DiD regression model:

$$Y = \beta_0 + \beta_1 * \text{Time} + \beta_2 * \text{Treatment} + \beta_3 * \text{Time} * \text{Treatment} + \varepsilon$$

where Y is the log-transformed seasonal pollutant average, Time is a dummy variable indicating whether the season is winter or spring, Treatment is a dummy variable indicating intervention or control group (i.e., year 2020 or 2019), and Time*Treatment is the interaction between time and treatment.

In addition to analyses of citywide seasonal averages, we stratified DiD analyses of NYCCAS $PM_{2.5}$ and NO_2 by neighborhood poverty level, $PM_{2.5}$-attributable hospital admissions for respiratory disease, and $PM_{2.5}$-attributable emergency department visits for asthma to quantify how changes in air quality during the shutdown varied among different populations within NYC. Modified Zip Code Tabulation Areas (modZCTA) were used as the neighborhood boundaries for these analyses. ModZCTAs are based on the U.S. Census Zip Code Tabulation Areas (ZCTA) and are defined using an algorithm that combines ZCTAs having populations below 30,000 with demographically similar neighboring ZCTAs to ensure stable rate calculations and reduce disclosure risk (NYC Department of Health and Mental Hygiene, unpublished methodology, 2016). Neighborhood poverty was calculated using the 2015-2019 American Community Survey and classified into four levels based on the percent of population residing under the federal poverty threshold: low poverty (<10%), medium poverty (10-20%), high poverty (20-30%), and very high poverty (>30%). Rates of $PM_{2.5}$-attributable health outcomes were derived for each modZCTA using a method described in a prior study (Kheirbek et al. 2013). A summary of this method is also provided in the supplementary information (Section S1). Rates of hospital admissions for respiratory disease in each modZCTA were calculated for adults 20 years of age and older, then grouped into tertiles (low: <8.4 per 100,000; medium: 8.4-12 per 100,000; high: >12 per 100,000) for stratification of DiD analyses. Rates of emergency department visits for asthma in each modZCTA were calculated for adults 18 years of age and older, then grouped into tertiles (low: <12.4 per 100,000; medium: 12.4-34 per 100,000; high: >34 per 100,000) for stratification of DiD analyses.

To evaluate model robustness, we performed two additional DiD regressions for each pollutant using NYCCAS data from 2016 - 2018 as alternative control groups. This serves as a check on the plausibility of the DiD estimate—if the intervention effect estimate is consistent across comparisons with multiple control groups, it makes it unlikely that an unusual event (weather or otherwise) biased our results. Additionally, we performed “placebo tests” (Lechner, 2010), where we assigned NYCCAS data from 2019 as a placebo treatment group and performed DiD regression for each pollutant using NYCCAS data from 2016 – 2018 as control groups. This serves as a check on the parallel trend assumption underlying the DiD model. If the treatment effect estimate from a model using a “placebo treatment” is statistically significant, then the parallel trends assumption does not hold. In other words, it suggests that the pollutant trends in the pre-intervention period are not constant over time and DiD analyses using these control groups would be biased and unable to capture the causal effect of the intervention (Dimick and Ryan 2014). Furthermore, DiD regression was performed using the temporally-resolved NYS DEC dataset for comparison to estimates from analysis of NYCCAS data. This temporally-resolved data set allowed us to use the exact dates of NY Pause and re-opening to assign intervention periods. Citywide daily average $PM_{2.5}$ and NO_2 concentrations were calculated from hourly measurements at the NYS DEC monitors following a method described in prior studies (Schwartz 2000, Strickland et al. 2011) for four different periods: Winter 2020 (1/1/20 – 3/19/20), Spring 2020 (3/20/20 – 6/7/20), Winter 2019 (1/1/19 – 3/19/19), and Spring 2019 (3/20/19 – 6/7/19). DiD analysis of hourly data was limited to monitors with at least 18 hours of data collected per day and at least 75% complete monitoring days out of the total number of days in each of the four study periods. After applying completeness criteria, eight $PM_{2.5}$ and two NO_2 monitoring sites remained for DiD estimation (Fig. S3). If multiple monitors are present at a given site, the measurements from the different monitors are averaged. DiD regression was then performed as described above using data from these four periods.

2.5. Spatial interpolation

Spatial patterns of $PM_{2.5}$ and NO_2 were analyzed using NYCCAS integrated measurements taken from 93 sites. Land-use regression models were developed to predict pollutant concentrations for each season in 2019 and 2020 at the centroids of 100m x 100m grid cells across the city. Forward stepwise model selection was employed to fit LUR models for each year of sampling with the blank-corrected pollutant measurements at the monitored sites as the dependent variable and emissions indicators as the predictor variables. Emissions indicators were entered into the model in order of their perceived a priori importance as described in Clougherty et al. (2013). The criteria for an indicator to be retained in the models are: (1) it yields a positive regression coefficient; (2) it is significant at $\alpha = 0.05$; (3) it increases the model R^2 by at least 2% from the previous model; and (4) it yields a model with variance inflation factors for all covariates that do not exceed 1.5. Smoothing terms for xy coordinates and unique sampling session ID were included to adjust for spatial autocorrelation and seasonality of pollutant concentrations, respectively. The spatial smooth term was given up to 10 degrees of freedom, and the temporal smooth term was given up to 24 degrees of freedom. The spatial smooth and each emission indicator in the model were included as interaction terms with unique season IDs to account for seasonal variations in spatial patterns and covariate effect size. Cook's Distance was also calculated for each model to determine if any outlier points had outsized influence on the model (Cook's Distance >1). If any sites were found to be "influential," model selection was repeated with these sites omitted, and the final models did not include these sites. To evaluate model robustness, we performed k-fold cross validation, where k = 10, and computed the normalized mean squared error (NMSE) of the k-fold cross validation models. Additionally, pollutant concentrations were predicted at the 100m x 100m grid cells using only the temporal and spatial smooth terms to assess how well the LUR predictions reflect the observed spatial patterns.

3. Results and discussion

3.1. Citywide air quality changes during NY Pause

Air pollution has been steadily decreasing in NYC and across the United States in recent years due to regulations, such as mandatory low-sulfur fuels for mobile vehicles and building boilers, and economic factors, such as declining costs of natural gas relative to coal (Pitiranggon et al. 2021, Rattigan et al. 2016, Squizzato et al. 2018, van Donkelaar et al. 2019). Thus, we implemented DiD regression of citywide average $PM_{2.5}$ and NO_2 to estimate whether any change in air pollution observed during the COVID-19 shutdown in NYC could be attributed to shifts in activity during the shutdown, apart from external trends, such as seasonality and long-term trends due to the aforementioned regulations and economic factors. DiD analyses of citywide seasonal averages measured at the 93 NYCCAS integrated sites show that the geometric mean of $PM_{2.5}$ decreased by 25% ($p < 0.001$, 95% CI [-33.7, -15.5]) and the geometric mean of NO_2 decreased by 29% ($p < 0.001$, 95% CI [-37.0, -20.1]) as a result of NY Pause. Fig. 2 shows the seasonal average $PM_{2.5}$ and NO_2 at the 93 NYCCAS integrated monitoring sites in NYC and their 95% confidence intervals during the winter and spring periods of 2019 and 2020. Placebo analysis shows no significant "treatment" effect when NYCCAS data from 2019 is assigned as a placebo treatment group and compared to NYCCAS data from 2016 - 2018 as control groups in a DiD regression. This suggests that our data do not violate the parallel trend assumption. To further evaluate the plausibility of our results, we compared DiD estimates using NYCCAS data to estimates from DiD models using the hourly NYS DEC data in which we were able to set study periods that lined up more precisely with specific intervention dates. Results from NYCCAS data are reasonably similar to, though somewhat higher than, results from NYS DEC data (18% reduction in $PM_{2.5}$ and 27% reduction in NO_2). This may be because NYCCAS monitors capture a wider range of emissions trends in the city, particularly in historically higher emission areas such as the CBD. Further details on our DiD regression of NYC DEC data are in Table S2 and Fig. S3.

Our results are also comparable to a prior study in NYC using NYS DEC hourly data (Perera et al. 2021), which reports a 23% decline in $PM_{2.5}$ and 34% decline in NO_2 during the shutdown compared to the 2015-2018 average over the same months. The NYS DEC network has relatively few monitoring sites, and the greater spatial resolution of the NYCCAS data used in our analysis gives greater confidence that our estimates are representative of changes across the entire city. Furthermore, our use of a causal inference method allowed us to estimate the changes that are attributable to the COVID-19 shutdown. Using a time-lagged linear regression model, Zangari et al. (2020) observed no significant difference in the rates of change in daily average NO_2 and $PM_{2.5}$ from January - early May 2020 compared to the same period in years prior (2015-2019), concluding that shutdown measures did not result in significant reductions in these pollutants in NYC. However, this study only examined the first 17 weeks of the year; thus, the model input included about twice as many days in the pre-shutdown period as in the shutdown period, perhaps biasing the model coefficients toward the pre-shutdown observations. Our DiD models incorporate data from 182 days each in the control and intervention periods, with a similar number of days in the winter and spring sessions of each period.

Our DiD estimates of citywide changes due to NY Pause are consistent with estimates from DiD models using NYCCAS data from 2016 – 2018 as alternative control groups (28% reduction in $PM_{2.5}$; 33-37% reduction in NO_2). Additional details of alternative model results are shown in Table S3. That the intervention effect estimate is consistent across comparisons with multiple control groups from different years makes it unlikely that an unusual event (weather or otherwise) biased our results. We also examined temperature, relative humidity,

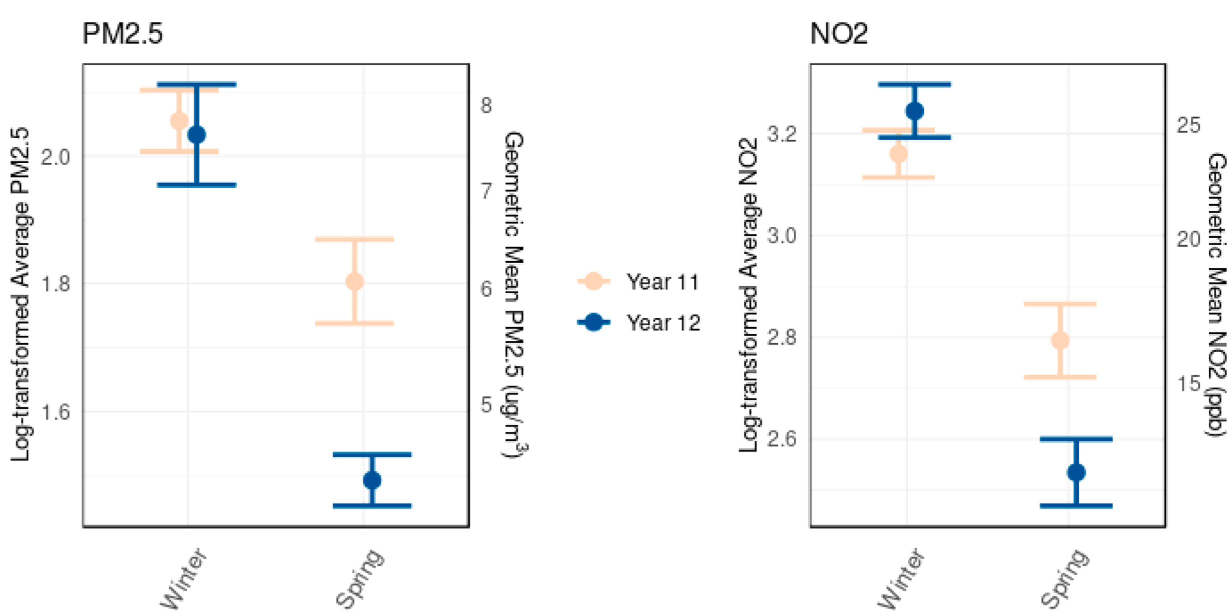

Fig. 2. Seasonal average $PM_{2.5}$ and NO_2 and 95% confidence intervals at 93 NYCCAS integrated monitoring sites in Winter and Spring of NYCCAS Years 11 and 12 (Winter Year 11 = Winter 2018-2019; Winter Year 12 = Winter 2019-2020; Spring Year 11 = Spring 2019; Spring Year 12 = Spring 2020).

precipitation, and wind speed measurements from LGA during the winter and spring periods of 2019 and 2020 to ascertain any meteorological effects on the observed changes in air pollution. Daily average temperature, relative humidity, precipitation, and wind speeds measured at LGA during the winter and spring periods of 2020 were compared to the same periods in 2019 (Fig. S4). T-tests show no significant difference at the 95% confidence level in weather parameters between 2019 and 2020 periods except for temperature in the winter periods. Temperatures were, on average, 4°F lower ($p < 0.001$, 95% CI [-6.5, -2.0]) in Winter 2018 - 2019 compared to Winter 2019 - 2020. Temperature may be positively or negatively associated with $PM_{2.5}$ levels due to the many distinct processes that contribute to $PM_{2.5}$ formation (NARSTO 2004, Wang and Ogawa 2015). However, a colder winter could lead to higher $PM_{2.5}$ and NO_2 levels due to greater emissions from home heating and the temperature inversions favored by cold winter weather (Beard et al. 2012, Janhäll et al. 2006, Navinya et al. 2020). Our DiD estimate is a measure of whether the reduction in air pollution from winter to spring in 2020 was greater than the reduction from winter to spring in 2019. If the colder winter in 2019 resulted in higher pollution than there would have been otherwise, this would have resulted in a larger reduction in pollution in the 2019 winter to spring transition, and, thus, a smaller DiD estimate. In other words, the colder winter in 2019 may have attenuated our DiD effect estimates. Thus, our findings suggest that our estimates of changes in air pollution due to the COVID-19 shutdown are not likely to have been biased in the direction of our findings by unusual weather in the control or intervention groups.

3.2. Spatial patterns of $PM_{2.5}$ and NO_2

Spatial patterns of air pollution interpolated from NYCCAS integrated $PM_{2.5}$ and NO_2 measurements reveal changes in local pollutant emissions following the COVID-19 shutdown. The spatial patterns predicted by the LUR models (Fig. 3(a-b), Fig. S5) generally agreed with those predicted from models that only included the temporal and spatial smooth terms (Fig. S6, Fig. S7), except that the LUR surfaces show more discrete pollution hotspots. This suggests that the LUR predictions reflect the observed spatial patterns of $PM_{2.5}$ and NO_2 and that the data on emissions indicators at the 100m x 100m grid cells allow for more highly-resolved predictions compared to pure spatial interpolation of temporally-adjusted measurements. The $PM_{2.5}$ predictors chosen via forward stepwise model selection are as follows: (1) number of permitted commercial char broilers less the number of precipitators within 1000m, (2) area of industrial land use within 1000m, and (3) traffic density weighted by relative $PM_{2.5}$ emissions by vehicle type within 250m. The NO_2 predictors chosen via forward stepwise model selection are as follows: (1) area of industrial land use within 1000m, (2) traffic density weighted by relative NO_x emissions by vehicle type within 100m, (3) whether a site is located within 100 feet of a bus route, (4) area of interior building space within 1000m, and (5) percent impervious surface within 100m. Tables S4 and S5 show the regression coefficients and their standard errors along with the effective degrees of freedom (EDF) of the temporal smooth terms and spatial smooth terms adjusted for seasonal interaction effects for each pollutant LUR model. k-Fold cross validation produced NMSEs of 0.23 and 0.21 for the 2019 and 2020 $PM_{2.5}$ LUR models, respectively. The NMSEs for the 2019 and 2020 NO_2 models are 0.17 and 0.18, respectively. All model residuals were approximately normally distributed.

The spatial distribution of LUR-predicted differences in $PM_{2.5}$ in Spring 2019 compared to Spring 2020 show that emissions decreased disproportionately in historically high-emission areas, such as the CBD, during the COVID-19 shutdown (Fig. 3a). To quantify how changes in $PM_{2.5}$ during the shutdown varied among neighborhoods experiencing

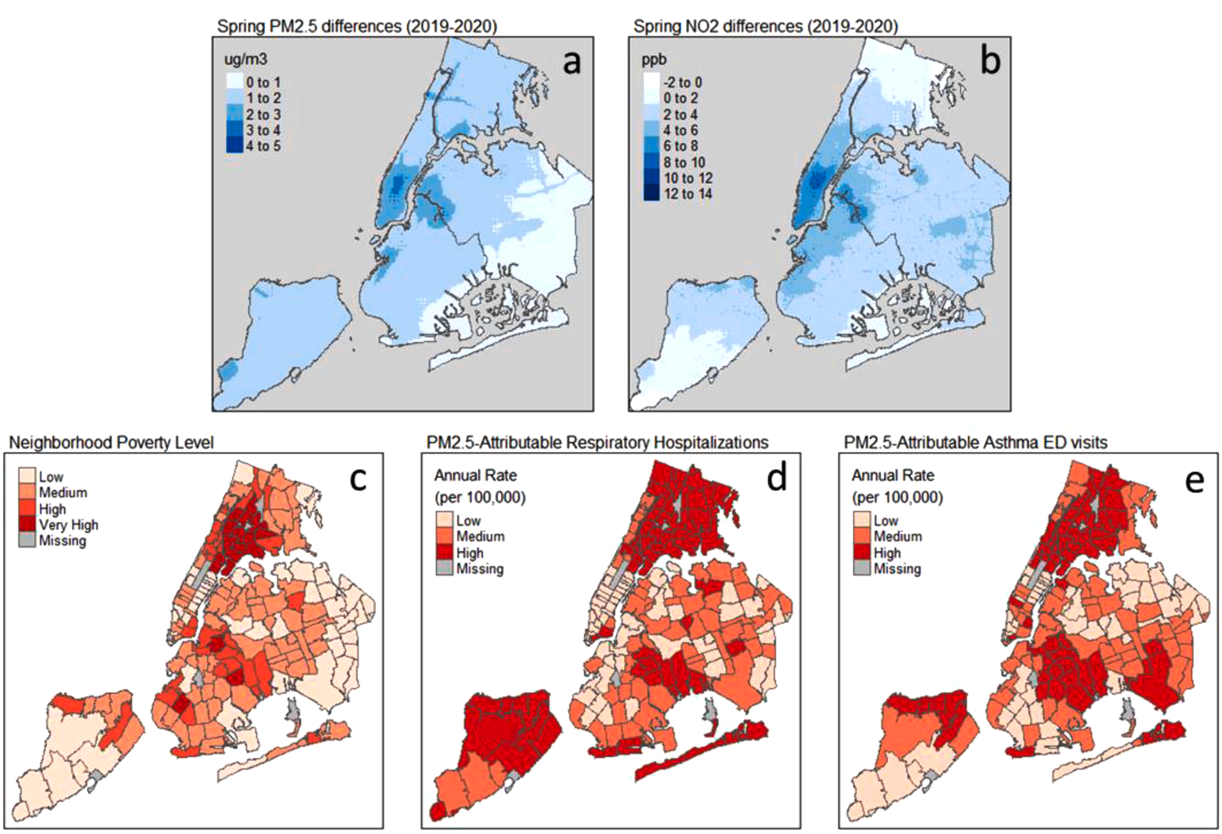

Fig. 3. Predicted changes in (a) $PM_{2.5}$ and (b) NO_2 at 100m x 100m grid cells in spring 2020 compared to spring 2019 from land-use regression modeling. Positive differences indicate lower concentrations in 2020 relative to 2019 values. Neighborhood (modZCTA) differences in (c) poverty level, (d) $PM_{2.5}$-attributable rates of hospitalization for respiratory disease, and (e) $PM_{2.5}$-attributable rates of emergency department visits for asthma.

different levels of poverty and different rates of $PM_{2.5}$-attributable health outcomes, we stratified DiD analysis of data from NYCCAS monitors in 2019 and 2020 by four different levels of poverty and by each tertile of $PM_{2.5}$-attributable rates of hospital admissions for respiratory disease and emergency department visits for asthma in each of the modZCTAs of NYC. The spatial distribution of these population characteristics is displayed in Fig. 3(c-e). In our analysis of neighborhoods with different levels of poverty (Fig. 4a), we only observed significant changes in $PM_{2.5}$ due to NY Pause in neighborhoods classified as medium poverty (36% reduction, $p < 0.05$, 95% CI [-47.7, -22.3]). The changes in $PM_{2.5}$ in neighborhoods classified as low, high, and very high poverty were not statistically significant at the 95% confidence level in our DiD regression models. In our analysis of neighborhoods with different rates of $PM_{2.5}$-attributable hospital admissions for respiratory disease (Fig. 4c), we observed significant reductions in $PM_{2.5}$ among all three groupings (low, medium, and high). However, the largest reductions were observed in neighborhoods impacted by the lowest rates of this $PM_{2.5}$-attributable health outcome (35% reduction, $p < 0.05$, 95% CI [-51.0, -12.4]). We estimate a 23% reduction in $PM_{2.5}$ due to the shutdown in neighborhoods impacted by medium rates ($p < 0.05$, 95% CI [-37.1, -5.25]) and highest rates ($p <0.05$, 95% CI [-34.3, -9.48]) of $PM_{2.5}$-attributable hospital admissions for respiratory disease. Similarly, in our analysis of neighborhoods with different rates of $PM_{2.5}$-attributable emergency department visits for asthma (Fig. 4d), we observed significant reductions in $PM_{2.5}$ among all three groupings (low, medium, and high), though the largest reductions were observed in neighborhoods impacted by the lowest rates (38% reduction, $p < 0.05$, 95% CI [-56.6, -10.7]), followed by those impacted by medium rates (29% reduction, $p < 0.001$, 95% CI[-40.7, -14.3]) and highest rates (18% reduction, $p < 0.05$, 95% CI[-30.2, -3.66]). These results show that

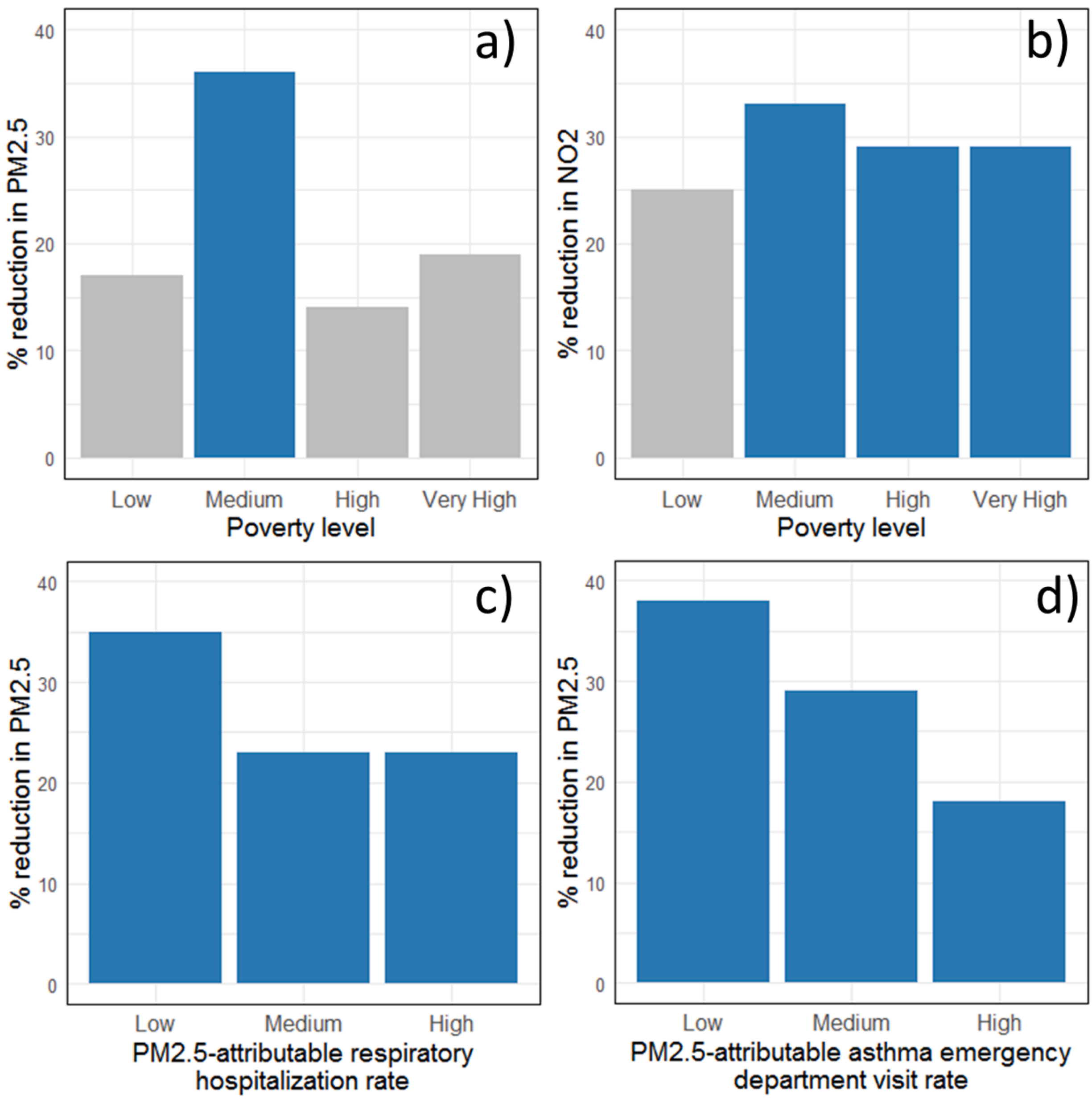

Fig. 4. Estimated reductions in pollution due to NY Pause stratified by neighborhood (modZCTA) characteristics. Estimates that are not statistically significant at the 95% confidence level are shown as gray bars. All other estimates were found to be statistically significant. (a) Reductions in $PM_{2.5}$ among neighborhoods with varying levels of poverty (b) Reductions in NO_2 among neighborhoods with varying levels of poverty (c) Reductions in $PM_{2.5}$ among neighborhoods with varying rates of $PM_{2.5}$-attributable hospital admissions for respiratory disease (d) Reductions in $PM_{2.5}$ among neighborhoods with varying rates of $PM_{2.5}$-attributable emergency department visits for asthma.

improvements in $PM_{2.5}$ pollution were not equitably distributed among the different populations of NYC. Moreover, these improvements tended to be smaller in neighborhoods that are the most highly burdened by poverty and $PM_{2.5}$-attributable health outcomes.

Spatial patterns of NO_2 indicate that some parts of the city, such as the CBD, experienced greater reductions during NY Pause (Fig. 3b). To quantify how changes in NO_2 during the shutdown varied among neighborhoods experiencing different levels of poverty, we stratified DiD analysis of data from NYCCAS monitors in 2019 and 2020 by four different levels of poverty attributed to the modZCTAs of NYC. We did not have neighborhood-level data on NO_2-attributable health outcomes for use in this study. We observed significant changes in NO_2 among all neighborhood poverty levels, except those classified as low poverty (Fig. 4b). The largest reductions were observed in medium poverty neighborhoods (33% reduction, $p < 0.001$, 95% CI [-45.5, -18.9]), followed by very high (29% reduction, $p < 0.001$, 95% CI [-40.0, -15.1]) and high poverty (29% reduction, $p < 0.001$, 95% CI [-39.2, -16.5]). Unlike $PM_{2.5}$, changes in NO_2 due to the shutdown were more consistent across NYC neighborhoods. One possible explanation for this is that the major outdoor source for NO_2 is road traffic (Jarvis et al. 2010), which is more evenly distributed across the city than commercial cooking, a major source of $PM_{2.5}$ in NYC that is highly concentrated in the CBD (Fig. S2).

3.3. Temporal patterns of $PM_{2.5}$ and NO_2

While t-tests of temporally-adjusted $PM_{2.5}$ concentrations at NYCCAS sites (Table S6) show that $PM_{2.5}$ concentrations were not significantly different in Winter 2019 - 2020 (mean: 8.2 ug/m^3; SD: 3.2) compared to Winter 2018 - 2019 (mean: 8.0 ug/m^3; SD: 2.0), $PM_{2.5}$ was significantly lower ($p < 0.001$, 95% CI [-2.6, -1.2]) and less varied in Spring 2020 (mean: 4.5 ug/m^3; SD: 1.1) compared to Spring 2019 (mean: 6.4 ug/m^3; SD: 2.9). $PM_{2.5}$ remained significantly lower ($p < 0.05$, 95% CI [-2.5, -0.27]) in Summer 2020 (mean: 7.9 ug/m^3; SD: 1.3) compared to Summer 2019 (mean: 9.2 ug/m^3; SD: 4.9), suggesting that the reductions in $PM_{2.5}$ pollution observed during the lockdown were sustained after re-opening. By Fall 2020 (mean: 5.9 ug/m^3; SD: 2.0), however, $PM_{2.5}$ appears to have rebounded to levels comparable to what was observed in Fall 2019 (mean: 6.2 ug/m^3; SD: 2.1).

While t-tests of temporally-adjusted NO_2 concentrations at NYCCAS sites (Table S6) show that Winter 2019-2020 NO_2 (mean: 26.5 ppb; SD: 7.0) was significantly higher ($p < 0.05$, 95% CI [0.52, 4.1]) than Winter 2018-2019 NO_2 (mean: 24.2 ppb; SD: 5.2), NO_2 was significantly lower ($p < 0.001$, 95% CI [-5.6, -2.5]) and less varied across NYCCAS sites in Spring 2020 (mean: 13.3 ppb; SD: 4.3) compared to Spring 2019 (mean: 17.3 ppb; SD: 6.1). NO_2 in Summer 2020 (mean: 13.5 ppb; SD: 4.9) was significantly lower ($p < 0.05$, 95% CI [-3.9, -0.52]) than Summer 2019 (mean: 15.7 ppb; SD: 6.4); however, the mean difference among the summer seasons was about half as much as that observed among the spring seasons. By Fall 2020, NO_2 at the NYCCAS sites (mean: 18.1 ppb; SD: 4.9) were no longer significantly different from the measurements from the prior fall (mean: 17.9 ppb; SD: 4.9). This data suggests that, on average, citywide NO_2 and $PM_{2.5}$ emissions more or less returned to business-as-usual by Fall 2020.

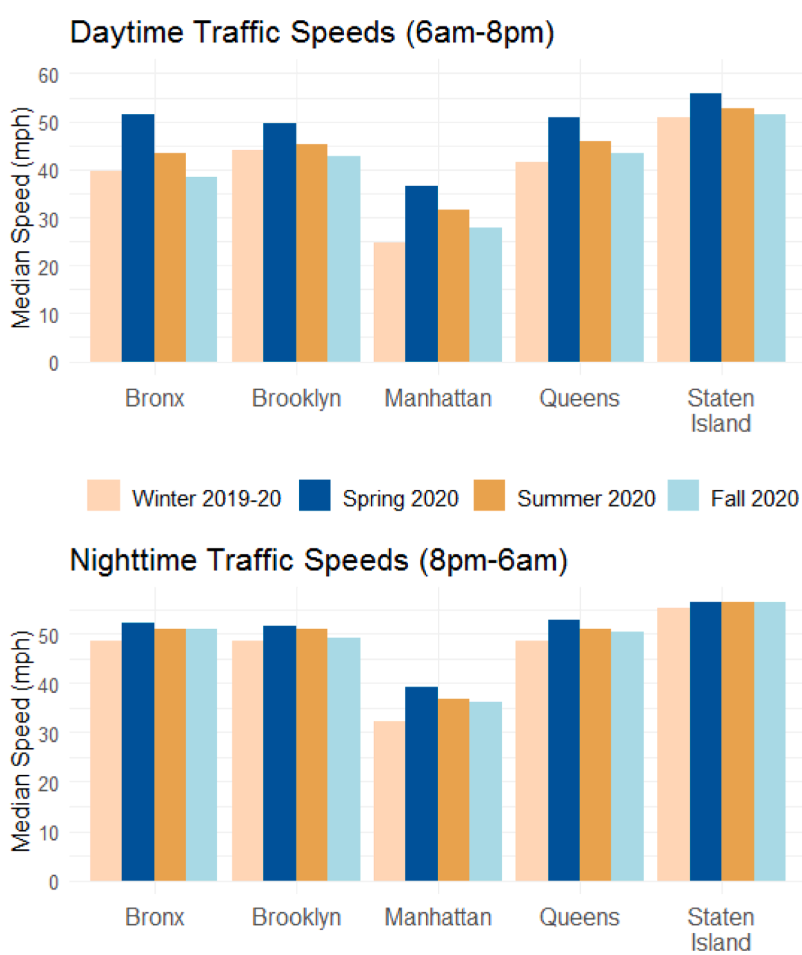

Fig. 5. Median traffic speeds (speeds of 0 excluded) along road links monitored by the NYC Department of Transportation in each of the five boroughs of NYC across four periods in Year 12 of the NYCCAS program.

3.4. Traffic

The NY Pause executive order included stay-at-home orders, directing individuals to limit outdoor recreational activities and use of public transportation (NYS Department of Health, 2020). This likely had the effect of reducing traffic activity across New York. Fig. 5 shows that average "daytime" (6am-8pm) traffic speeds in Spring 2020 were faster compared to Winter 2019 - 2020 across the road links monitored by the NYC Department of Transportation (NYC Department of Transportation (NYC DOT) 2021), suggesting widespread decreases in daytime traffic in NYC during the shutdown. Figure S8 shows changes at the individual links monitored by the NYC DOT. This is corroborated by the reduced

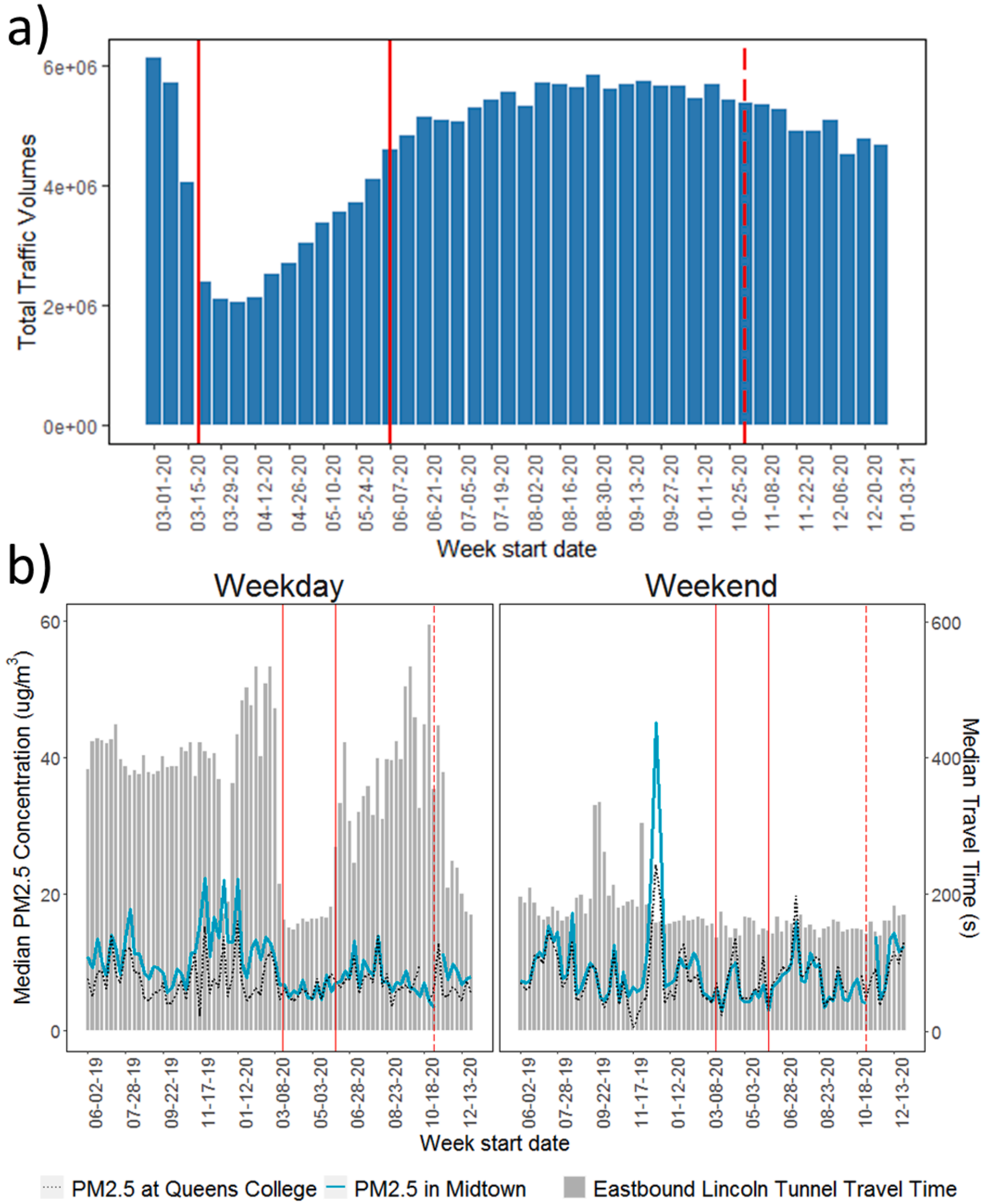

Fig. 6. a) Weekly traffic volumes at MTA Bridges and Tunnels crossings during all times of day (https://new.mta.info/coronavirus/ridership) b) Weekly averages of morning (6am-9am) $PM_{2.5}$ in midtown Manhattan (black dotted line) and the Queens College urban background site (blue line) and traffic speeds on the Eastbound Lincoln Tunnel in midtown Manhattan (gray bars). Travel times of 0 excluded. Solid red vertical lines mark start/end of NY Pause. Dashed red vertical lines mark the approximate start date (11/1/20) of fall resurgence in NYC COVID-19 cases (https://www1.nyc.gov/site/doh/covid/covid-19-data-trends.page).

congestion observed in Manhattan (Shearston et al. 2021) and decreased traffic volumes observed citywide at MTA Bridges and Tunnels (Metropolitan Transportation Authority 2021) crossings during NY Pause (Fig. 6a). The decline is particularly evident in commuter traffic patterns (Fig. 6b). Morning rush hour travel times on the Eastbound Lincoln Tunnel, the peak morning commute direction because it leads into midtown Manhattan, which is in the CBD (Fig. 1), decreased by 45% during Spring 2020 relative to Winter 2019 - 2020. Reduction in Eastbound Lincoln Tunnel traffic during NY Pause coincided with a convergence of $PM_{2.5}$ levels at the nearby Midtown-DOT NYCCAS hourly $PM_{2.5}$ monitoring site with the hourly $PM_{2.5}$ monitoring site at Queens College, which is our designated urban background site (Fig. 6b). Fig. 1 displays the locations of traffic and pollution monitoring sites named in this section. “Nighttime” (8pm – 6am) traffic speeds did not increase as much as “daytime” traffic speeds (Fig. 5), perhaps because of the influence of road freight transport on overnight traffic (Shearston et al. 2020). Road freight transport (i.e., delivery trucks) may not have declined as much as commuter traffic, and it may have even increased, given increased online shopping during the COVID-19 shutdown (Zipkin 2020).

Citywide, Summer 2020 traffic speeds generally remained faster than Winter 2019 - 2020 speeds; however, the magnitude of the changes was weaker than those observed during Spring 2020 (Figs. 5, S8). Citywide traffic speeds in Fall 2020 were still faster than in Winter 2019 - 2020 in some parts of the city, such as the CBD, though the magnitude of change continued to weaken, and many road links exhibited slower speeds in Fall 2020 compared to Winter 2019 - 2020 (Figs. 5, S8). While morning rush travel times on the Eastbound Lincoln Tunnel increased following Phase 1 reopening in early June, the convergence of $PM_{2.5}$ at the midtown and urban background sites observed during the shutdown was sustained even after this rebound in traffic (Fig. 6b), implicating a reason other than traffic for observed $PM_{2.5}$ reductions in midtown Manhattan. Interestingly, travel times during morning rush on the Eastbound Lincoln Tunnel fell again in November following the resurgence of COVID-19 cases at around the same time in NYC (Fig. 6b). This steep decline in travel time observed during morning rush in midtown (on the Eastbound Lincoln Tunnel) following the fall 2020 increase in COVID-19 cases was not accompanied by a proportionate decline in citywide traffic volumes, at all times-of-day, at the MTA Bridges and Tunnels crossings (Fig. 6a), suggesting that commuter traffic activity was more sensitive to change during the resurgence than other types of traffic.

3.5. *Commercial cooking*

In addition to the stay-at-home order, the NY Pause executive order shut down all non-essential businesses statewide and banned non-essential gatherings of any size, including in-person dining in restaurants (Gold and Stevens 2020, NYS Department of Health, 2020). Commercial activity and commercial cooking, in particular, are major sources of air pollution in NYC (Clougherty et al. 2013, Ito et al. 2016). The 2017 National Emissions Inventory (NEI) attributes nearly 40% of local $PM_{2.5}$ emissions in NYC to commercial cooking (US Environmental Protection Agency, 2017). During the shutdown, the number of small businesses that were open in NYC was, on average, 45% lower compared to January 2020 (Opportunity Insights 2021). The percent change in the number of small businesses in the leisure and hospitality sector operating in NYC during the shutdown was even greater, with an average decrease of 54%. A borough-level breakdown of small business activity shows that Manhattan, where the CBD is located, experienced a greater percent decrease (53%) during the shutdown compared to the other boroughs (32 – 43%) (Opportunity Insights 2021). Given its large contribution to $PM_{2.5}$ pollution in NYC and the magnitude of decline in business in the leisure and hospitality sector following restrictions on restaurants, reduced commercial cooking activity is a likely cause for observed decreases in $PM_{2.5}$. This is further evidenced by the disproportionate decreases in $PM_{2.5}$ observed in the CBD, where there is a high density of commercial cooking establishments (Fig. S2). It is often difficult to geographically disentangle commercial cooking emissions from building emissions (i.e., boiler emissions), since areas with a high density of restaurants also tend to have a high density of built space (Fig. S2). However, the sustained reductions in $PM_{2.5}$ in the CBD during Summer 2020, even as traffic rebounded, points to commercial cooking as a major reason for this change, as building boiler emissions become less significant in the hotter months when indoor heating is unnecessary. Furthermore, public data shows that the number of small businesses in leisure and hospitality operating in NYC remained, on average, 47% lower (daily range: -53% to -43%), compared to January 2020, after reopening through the end of 2020 (Opportunity Insights 2021).

3.6. *Building boilers*

Another major source of air pollution in NYC is emissions from heating fuel combustion for building boilers, especially in the winter and early spring months. With more people staying home as well as decreased business activity during the shutdown, the effect of NY Pause on this source is harder to ascertain than with other major emission sources. An examination of NYS heating fuel consumption (US Energy Information Administration 2020) suggests that emissions from this source did not decrease following the shutdown (Table S7). Monthly No. 2 fuel oil sales (thousand gallons per day) in April-June 2020 ranged from 22% – 48% higher than the same time in 2019. By comparison, 2020 sales were 1% - 8% lower in January – March, compared to 2019 sales. While these data include fuel oil sales for all of New York State, NYC is a major consumer of fuel oil within the state, so these data likely reflect the trends in NYC (New York State Energy Research and Development Authority, 2021). These data suggest that changes in building heating activity did not contribute to the observed air quality improvements during NY Pause.

3.7. *Policy implications*

Our LUR models suggest that there are three major categories of sources of $PM_{2.5}$ and NO_2 in NYC—traffic, commercial cooking, and building boiler emissions for heat and hot water. Our examination of local emissions from these sources during the COVID-19 shutdown in NYC suggests that decreased traffic and commercial cooking activity resulted in significant reductions in $PM_{2.5}$ and NO_2. Therefore, this study gives a sense of what can be expected from policies that regulate traffic and commercial cooking in NYC. Though air pollution declined throughout the city during NY Pause, our LUR models show that the reductions were most pronounced in the CBD (Fig. 3(a-b)). The spatial distribution of these benefits is important to note because most of the NYC neighborhoods with the highest rates of air pollution attributable health outcomes are outside of the CBD (Fig. 3(d-e), Kheirbek et al. 2013, NYC Department of Health and Mental Hygiene (NYC DOHMH) 2021b). In our analysis of changes in air pollution during NY Pause among neighborhoods experiencing varying levels of poverty and $PM_{2.5}$-attributable health outcomes, we found uneven reductions in $PM_{2.5}$ across these different populations. Improvements in $PM_{2.5}$ pollution tended to be smaller in neighborhoods that are the most highly burdened by poverty and $PM_{2.5}$-attributable health outcomes. NO_2 reductions due to the shutdown were more evenly distributed across different demographic groups, perhaps because the major outdoor source for NO_2 is road traffic (Jarvis et al. 2010), which is more evenly distributed across the city than commercial cooking, a major source of $PM_{2.5}$ in NYC that is highly concentrated in the CBD (Fig. S2). While traffic is also a source of $PM_{2.5}$, truck traffic (i.e., road freight transport) may not have decreased as much as car traffic, or it may have even increased, due to increased online shopping during the COVID-19 shutdown (Zipkin 2020). Trucks emit more $PM_{2.5}$ per mile compared to cars (Bureau of Transportation Statistics, 2021). This suggests that regulations on citywide car traffic would have a greater impact on NO_2 compared to $PM_{2.5}$ and that regulation of commercial cooking emissions has greater potential to reduce $PM_{2.5}$, especially in the CBD. As with COVID-19 and other public health crises, air pollution and diseases related to air pollution disproportionately affect underprivileged populations (Bozack et al. 2021, Johnson et al. 2020, Rozenfeld et al. 2020, Tessum et al. 2021, Thakur et al. 2020). Though pollution reductions anywhere are beneficial for both health and environmental reasons, we must be sure to enact policy that prioritizes those who suffer most from pollution-related health impacts. For example, we can aim to reduce the air quality impacts of truck and bus traffic in high-poverty neighborhoods, which are known to bear the greatest burden of $PM_{2.5}$ exposure and $PM_{2.5}$-attributable health outcomes from these sources (Kheirbek et al. 2016).

3.8. Strengths and limitations

A strength of this study is the NYCCAS network's high-density of long-term, ground-level air pollution monitors. This gives us the ability to show highly-resolved changes in spatial patterns before, during, and after the COVID-19 shutdown, which no other studies of NYC, to our knowledge, have been able to do using exposure-relevant, direct ground observations. DiD analysis of NYCCAS seasonal averages gives us an estimate of the shutdown's effect on $PM_{2.5}$ and NO_2 levels in NYC that is more representative of changes across the entire city than estimates using the sparser NYS DEC regulatory monitoring network. Furthermore, the high spatial density of the NYCCAS network has allowed us to quantify how changes in air quality during the shutdown varied among different demographic groups within NYC. One weakness of NYCCAS integrated data is its temporal resolution, which is limited to seasonal averages at each site. This limited our ability to divide study periods precisely according to the timeline of events during the pandemic. However, the fact that our DiD estimates produced from NYCCAS data were reasonably comparable to our DiD estimates produced from hourly NYS DEC data suggests that the NYCCAS sampling seasons adequately overlap with the pre-shutdown and shutdown periods. Changes in pollution-emitting activity in NYC did not happen in a vacuum, as other municipalities also implemented lockdown measures to prevent the spread of COVID-19 at around the same time. Even so, the changes in spatial distribution of $PM_{2.5}$ and NO_2 apparent from the NYCCAS monitors suggest that local emission reductions contributed significantly to the observed decline in pollution. The correlation between the emissions indicators used in this paper and observed changes in air pollution does not prove causality. However, given prior findings on major air pollution sources in NYC from LUR and other source apportionment studies (Masiol et al. 2017, NYC Department of Health and Mental Hygiene (NYC DOHMH) 2021c, Sun et al. 2011), as well as what we know about the industries affected by the COVID-19 shutdown, the trends reported here indicate a plausible link between changes in economic activity and air pollution as a result of shutdown measures.

4. Conclusions

Our analysis indicates that the COVID-19 shutdown in NYC resulted in a 25% reduction in citywide average $PM_{2.5}$ and a 29% reduction in citywide average NO_2 and that these changes are significant even after considering meteorology and long-term trends. An assessment of local pollution source activity suggests that decreases in commercial cooking and traffic contributed to observed declines in air pollution; thus, this study shows the potential for regulations on traffic and commercial cooking to reduce air pollution in NYC. Pollutant reductions occurred disproportionately in the CBD, with smaller changes in the parts of the city that experience the highest burden of poverty and air pollution-related health impacts. Any future studies on the pollution effects of regulations on commercial cooking or traffic, such as congestion pricing (Fix NYC Panel 2018), should be sure to examine both the magnitude and equity of impact. Further research could increase understanding of how changes in source activity affected air pollution during the COVID-19 shutdown by examining spatial patterns of pollution sources at higher resolution using crowd-sourced data (Hilpert et al. 2021) or chemical source apportionment (Ito et al. 2016). The extreme toll that the pandemic has taken on lives and livelihoods far outweighs any health benefits from concurrent reductions in pollution, which for the most part seemed to rebound to business-as-usual levels by Fall 2020. However, we can use what we have learned from this experience to inform effective and equitable environmental health policy.

CRediT authorship contribution statement

Masha Pitiranggon: Methodology, Formal analysis, Visualization, Writing – original draft. **Sarah Johnson:** Conceptualization, Methodology, Writing – review & editing, Supervision. **Christopher Huskey:** Data curation, Writing – review & editing. **Holger Eisl:** Investigation, Writing – review & editing. **Kazuhiko Ito:** Methodology, Writing – review & editing, Supervision.

Declaration of interests

The authors declare that they have no known competing financial interests or personal relationships that could have appeared to influence the work reported in this paper.

Acknowledgements

We thank Joseph Osso and Matthew Milford at NYSERDA for pointing us to the New York State fuel oil sales data. Previous versions of the manuscript were improved by thoughtful comments from Carolyn Olson (NYC Department of Health and Mental Hygiene), Nalyn Siripanichgon (Queens College), and two anonymous reviewers. This research was supported by the City of New York tax levy funds.

Supplementary materials

Supplementary material associated with this article can be found, in the online version, at doi:10.1016/j.envadv.2022.100171.

References

Adams, M.D., 2020. Air pollution in Ontario, Canada during the COVID-19 State of Emergency. Sci Total Environ 742, 140516.
Alexeeff, S.E., Liao, N.S., Liu, X., Van Den Eeden, S.K., Sidney, S., 2021. Long-Term PM2.5 Exposure and Risks of Ischemic Heart Disease and Stroke Events: Review and Meta-Analysis. J Am Heart Assoc 10 (1), e016890.
Atkinson, R.W., Butland, B.K., Anderson, H.R., Maynard, R.L., 2018. Long-term Concentrations of Nitrogen Dioxide and Mortality: A Meta-analysis of Cohort Studies. Epidemiology 29 (4), 460–472.
Beard, J.D., Beck, C., Graham, R., Packham, S.C., Traphagan, M., Giles, R.T., Morgan, J. G., 2012. Winter temperature inversions and emergency department visits for asthma in Salt Lake County, Utah, 2003-2008. Environ Health Perspect 120 (10), 1385–1390.
Berman, J.D., Ebisu, K., 2020. Changes in U.S. air pollution during the COVID-19 pandemic. Sci Total Environ 739, 139864.
Bozack, A., Pierre, S., DeFelice, N., Colicino, E., Jack, D., Chillrud, S. N.,.. & Lee, A. G. (2021). Long-Term Air Pollution Exposure and COVID-19 Mortality: A Patient-Level Analysis from New York City. *American Journal of Respiratory and Critical Care Medicine*, (ja).
Briz-Redon, A., Belenguer-Sapina, C., Serrano-Aroca, A., 2021. Changes in air pollution during COVID-19 lockdown in Spain: A multi-city study. J Environ Sci (China) 101, 16–26.
Bureau of Transportation Statistics, 2021. Estimated U.S. Average Vehicle Emissions Rates per Vehicle by Vehicle Type Using Gasoline and Diesel. Available online: https://www.bts.gov/content/estimated-national-average-vehicle-emissions-rates-vehicle-vehicle-type-using-gasoline-and.
Chen, K., Wang, M., Huang, C., Kinney, P.L., Anastas, P.T., 2020. Air pollution reduction and mortality benefit during the COVID-19 outbreak in China. The Lancet Planetary Health 4 (6), e210–e212.
Cho, S.I., Yoon, S., Lee, H.J., 2021. Impact of comorbidity burden on mortality in patients with COVID-19 using the Korean health insurance database. Scientific reports 11 (1), 1–9.

Civerolo, K.L., Rattigan, O.V., Felton, H.D., Schwab, J.J., 2017. Changes in Gas-Phase Air Pollutants across New York State, USA. Aerosol and Air Quality Research 17 (1), 147–166.
Clougherty, J.E., Kheirbek, I., Eisl, H.M., Ross, Z., Pezeshki, G., Gorczynski, J.E., Johnson, S., Markowitz, S., Kass, D., Matte, T., 2013. Intra-urban spatial variability in wintertime street-level concentrations of multiple combustion-related air pollutants: the New York City Community Air Survey (NYCCAS). J Expo Sci Environ Epidemiol 23 (3), 232–240.
Costa, S., Ferreira, J., Silveira, C., Costa, C., Lopes, D., Relvas, H., Borrego, C., Roebeling, P., Miranda, A.I., Teixeira, J.P., 2014. Integrating health on air quality assessment–review report on health risks of two major European outdoor air pollutants: PM and NO2. J Toxicol Environ Health B Crit Rev 17 (6), 307–340.
Dimick, J.B., Ryan, A.M., 2014. Methods for evaluating changes in health care policy: the difference-in-differences approach. Jama 312 (22), 2401–2402.
Fix NYC Panel (2018) Fix NYC Advisory Panel Report January 2018. Available online: https://www.scribd.com/document/369529810/Fix-NYC-Panel-Report.
Fu, F., Purvis-Roberts, K.L., Williams, B., 2020. Impact of the COVID-19 Pandemic Lockdown on Air Pollution in 20 Major Cities around the World. Atmosphere 11 (11).
Gold, M. and Stevens, M. (2020) What Restrictions on Reopening Remain in New York? New York Times. Available online: https://www.nytimes.com/article/new-york-phase-reopening.html.
He, G., Pan, Y., Tanaka, T., 2020. The short-term impacts of COVID-19 lockdown on urban air pollution in China. Nature Sustainability 3 (12), 1005–1011.
Hilpert, M., Shearston, J. A., Cole, J., Chillrud, S. N., & Martinez, M. E. (2021). Acquisition and analysis of crowd-sourced traffic data. arXiv preprint arXiv: 2105.12235.
Ito, K., Johnson, S., Kheirbek, I., Clougherty, J., Pezeshki, G., Ross, Z., Eisl, H., Matte, T. D., 2016. Intraurban Variation of Fine Particle Elemental Concentrations in New York City. Environ Sci Technol 50 (14), 7517–7526.
Janhäll, S., Olofson, K.F.G., Andersson, P.U., Pettersson, J.B., Hallquist, M., 2006. Evolution of the urban aerosol during winter temperature inversion episodes. Atmospheric Environment 40 (28), 5355–5366.
Jarvis, DJ, Adamkiewicz, G, Heroux, ME, et al., 2010. Nitrogen dioxide. WHO Guidelines for Indoor Air Quality: Selected Pollutants. World Health Organization, Geneva, p. 5. Available from: https://www.ncbi.nlm.nih.gov/books/NBK138707/.
Johnson, S., Haney, J., Cairone, L., Huskey, C., Kheirbek, I., 2020. Assessing Air Quality and Public Health Benefits of New York City's Climate Action Plans. Environ Sci Technol 54 (16), 9804–9813.
Ju, M.J., Oh, J., Choi, Y.H., 2021. Changes in air pollution levels after COVID-19 outbreak in Korea. Sci Total Environ 750, 141521.
Kerr, G.H., Goldberg, D.L., Anenberg, S.C., 2021. COVID-19 pandemic reveals persistent disparities in nitrogen dioxide pollution. In: Proceedings of the National Academy of Sciences, 118.
Kheirbek, I., Haney, J., Douglas, S., Ito, K., Matte, T., 2016. The contribution of motor vehicle emissions to ambient fine particulate matter public health impacts in New York City: a health burden assessment. Environ Health 15 (1), 89.
Kheirbek, I., Wheeler, K., Walters, S., Kass, D., Matte, T., 2013. PM2.5 and ozone health impacts and disparities in New York City: sensitivity to spatial and temporal resolution. Air Qual Atmos Health 6 (2), 473–486.
Le, T., Wang, Y., Liu, L., Yang, J., Yung, Y.L., Li, G., Seinfeld, J.H., 2020. Unexpected air pollution with marked emission reductions during the COVID-19 outbreak in China. Science 369 (6504), 702–706.
Lechner, M., 2010. The Estimation of Causal Effects by Difference-in-Difference Methods Estimation of Spatial Panels. Foundations and Trends® in Econometrics 4 (3), 165–224.
Liang, D., Shi, L., Zhao, J., Liu, P., Sarnat, J.A., Gao, S., Chang, H.H., 2020. Urban air pollution may enhance COVID-19 case-fatality and mortality rates in the United States. The Innovation 1 (3), 100047.
Masiol, M., Hopke, P.K., Felton, H.D., Frank, B.P., Rattigan, O.V., Wurth, M.J., LaDuke, G.H., 2017. Source apportionment of PM2.5 chemically speciated mass and particle number concentrations in New York City. Atmospheric Environment 148, 215–229.
Matte, T.D., Ross, Z., Kheirbek, I., Eisl, H., Johnson, S., Gorczynski, J.E., Kass, D., Markowitz, S., Pezeshki, G., Clougherty, J.E., 2013. Monitoring intraurban spatial patterns of multiple combustion air pollutants in New York City: design and implementation. J Expo Sci Environ Epidemiol 23 (3), 223–231.
Metropolitan Transportation Authority (2021) MTA service during the coronavirus pandemic. Available online: https://new.mta.info/coronavirus/ridership.
NARSTO (2004) Particulate Matter Science for Policy Makers: A NARSTO Assessment, Cambridge University Press, Cambridge, England.
Navinya, C., Patidar, G., Phuleria, H.C., 2020. Examining Effects of the COVID-19 National Lockdown on Ambient Air Quality across Urban India. Aerosol and Air Quality Research 20 (8), 1759–1771.
NYC Department of Health and Mental Hygiene (2021a) Appendix 1 - Sampling methodology and data sources for emissions indicators. Available online: https://nyccas.cityofnewyork.us/nyccas2021/web/sites/default/files/NYCCAS-appendix/Appendix1.pdf.
NYC Department of Health and Mental Hygiene (2021b) Health Impacts of Air Pollution. Available online: https://a816-dohbesp.nyc.gov/IndicatorPublic/Subtopic.aspx?theme_code=2,3&subtopic_id=103.
NYC Department of Health and Mental Hygiene (2021c). The New York City Community Air Survey: Neighborhood Air Quality 2008-2019. Available online: https://nyccas.cityofnewyork.us/nyccas2021/web/report.
NYC Department of Transportation (2021). DOT Traffic Speeds NBE. Available online: https://dev.socrata.com/foundry/data.cityofnewyork.us/i4gi-tjb9.
New York State Energy Research and Development Authority, 2021. Patterns and Trends. New York State Energy Profiles 2003–2017.
New York State (2021). Phase One Industries. Available online:https://forward.ny.gov/phase-one-industries.
NYS Department of Environmental Conservation (2021) Air Monitoring Website. Avaialble online: http://www.nyaqinow.net/.
NYS Department of Health (2020) New York State on PAUSE. Available online: https://coronavirus.health.ny.gov/new-york-state-pause.
Opportunity Insights (2021) Economic Tracker. Available online: https://github.com/OpportunityInsights/EconomicTracker/tree/main/data.
Orellano, P., Reynoso, J., Quaranta, N., Bardach, A., Ciapponi, A., 2020. Short-term exposure to particulate matter (PM10 and PM2.5), nitrogen dioxide (NO2), and ozone (O3) and all-cause and cause-specific mortality: Systematic review and meta-analysis. Environ Int 142, 105876.
Perera, F., Berberian, A., Cooley, D., Shenaut, E., Olmstead, H., Ross, Z., Matte, T., 2021. Potential health benefits of sustained air quality improvements in New York City: A simulation based on air pollution levels during the COVID-19 shutdown. Environ Res 193, 110555.
Pitiranggon, M., Johnson, S., Haney, J., Eisl, H., Ito, K., 2021. Long-term trends in local and transported PM2.5 pollution in New York City. Atmospheric Environment 248.
Rattigan, O.V., Civerolo, K.L., Felton, H.D., Schwab, J.J., Demerjian, K.L., 2016. Long Term Trends in New York: PM2.5 Mass and Particle Components. Aerosol and Air Quality Research 16 (5), 1191–1205.
Rozenfeld, Y., Beam, J., Maier, H., Haggerson, W., Boudreau, K., Carlson, J., Medows, R., 2020. A model of disparities: risk factors associated with COVID-19 infection. International journal for equity in health 19 (1), 1–10.
Schwab, J.J., Felton, H.D., Rattigan, O.V., Demerjian, K.L., 2006. New York State urban and rural measurements of continuous PM2.5 mass by FDMS, TEOM, and BAM. J Air Waste Manag Assoc 56 (4), 372–383.
Schwartz, J., 2000. The distributed lag between air pollution and daily deaths. Epidemiology 11 (3), 320–326.
Shearston, J.A., Johnson, A.M., Domingo-Relloso, A., Kioumourtzoglou, M.A., Hernández, D., Ross, J., Chillrud, S.N. and Hilpert, M., 2020. Opening a large delivery service warehouse in the South Bronx: impacts on traffic, air pollution, and noise. International journal of environmental research and public health 17 (9), 3208.
Shearston, J.A., Martinez, M.E., Nunez, Y., Hilpert, M., 2021. Social-distancing fatigue: evidence from real-time crowd-sourced traffic data. Science of The Total Environment, 148336.
Shehzad, K., Bilgili, F., Koçak, E., Xiaoxing, L., Ahmad, M., 2021. COVID-19 outbreak, lockdown, and air quality: fresh insights from New York City. Environmental Science and Pollution Research 1–13.
Song, J., Zeng, M., Wang, H., Qin, C., Hou, H.Y., Sun, Z.Y., Liu, Z., 2021. Distinct effects of asthma and COPD comorbidity on disease expression and outcome in patients with COVID-19. Allergy 76 (2), 483–496.
Squizzato, S., Masiol, M., Rich, D.Q., Hopke, P.K., 2018. PM2.5 and gaseous pollutants in New York State during 2005–2016: Spatial variability, temporal trends, and economic influences. Atmospheric Environment 183, 209–224.
Strickland, M.J., Darrow, L.A., Mulholland, J.A., Klein, M., Flanders, W.D., Windquist, A., Tolbert, P.E., 2011. Implications of different approaches for characterizing ambient air pollutant concentrations within the urban airshed for time-series studies and health benefits analyses. Environmental Health 10 (36), 1–9.
Sun, Y.L., Zhang, Q., Schwab, J.J., Demerjian, K.L., Chen, W.N., Bae, M.S., Hung, H.M., Hogrefe, O., Frank, B., Rattigan, O.V., Lin, Y.C., 2011. Characterization of the sources and processes of organic and inorganic aerosols in New York city with a high-resolution time-of-flight aerosol mass apectrometer. Atmospheric Chemistry and Physics 11 (4), 1581–1602.
Tessum, C.W., Paolella, D.A., Chambliss, S.E., Apte, J.S., Hill, J.D., Marshall, J.D., 2021. PM2. 5 polluters disproportionately and systemically affect people of color in the United States. Science Advances 7 (18), eabf4491.
Thakur, N., Lovinsky-Desir, S., Bime, C., Wisnivesky, J.P., Celedón, J.C., 2020. The structural and social determinants of the racial/ethnic disparities in the US COVID-19 pandemic. What's our role? American journal of respiratory and critical care medicine 202 (7), 943–949.
US Energy Information Administration (2020) New York No. 2 Fuel Oil Sales/Deliveries by Prime Supplier. Available online: https://www.eia.gov/dnav/pet/hist/LeafHandler.ashx?n=PET&s=C210012361&f=M.
US Environmental Protection Agency (2017) National Emissions Inventory. Available online: https://www.epa.gov/air-emissions-inventories/2017-national-emissions-inventory-nei-data#datas.
US Environmental Protection Agency (USEPA) (2019) Integrated Science Assessment for Particulate Matter.
US Environmental Protection Agency, 2016. Integrated Science Assessment for Oxides of Nitrogen -. Health Criteria.
van Donkelaar, A., Martin, R.V., Li, C., Burnett, R.T., 2019. Regional Estimates of Chemical Composition of Fine Particulate Matter Using a Combined Geoscience-Statistical Method with Information from Satellites, Models, and Monitors. Environ Sci Technol 53 (5), 2595–2611.
Venter, Z.S., Aunan, K., Chowdhury, S., Lelieveld, J., 2020. COVID-19 lockdowns cause global air pollution declines. Proc Natl Acad Sci U S A 117 (32), 18984–18990.
Wang, J., Ogawa, S., 2015. Effects of Meteorological Conditions on PM2.5 Concentrations in Nagasaki. Japan. Int J Environ Res Public Health 12 (8), 9089–9101.

Wu, X., Nethery, R.C., Sabath, M.B., Braun, D., Dominici, F., 2020. Air pollution and COVID-19 mortality in the United States: Strengths and limitations of an ecological regression analysis. Science advances 6 (45).
Zangari, S., Hill, D.T., Charette, A.T., Mirowsky, J.E., 2020. Air quality changes in New York City during the COVID-19 pandemic. Sci Total Environ 742, 140496.
Zipkin, A. (2020) As Online Buying Surges, So Do Noisy Cargo Flights. Available online: https://www.nytimes.com/2020/04/15/business/cargo-planes-deliveries-noise.html.